

# A Compact Switch by Tuning of Effective Thermo-optic Coefficient of Waveguide Supermodes

Jiapeng Luan

Department of Electronic Engineering  
The Chinese University of Hong Kong  
Shatin, N. T., Hong Kong, S. A. R.,  
China  
jpluan@link.cuhk.edu.hk

Yue Qin

Department of Electronic Engineering  
The Chinese University of Hong Kong  
Shatin, N. T., Hong Kong, S. A. R.,  
China  
YueQin-  
PotatoMaxwell@link.cuhk.edu.hk

Zelu Wang

Department of Electronic Engineering  
The Chinese University of Hong Kong  
Shatin, N. T., Hong Kong, S. A. R.,  
China  
1155184051@link.cuhk.edu.hk

Hon Ki Tsang

Department of Electronic Engineering  
The Chinese University of Hong Kong  
Shatin, N. T., Hong Kong, S. A. R.,  
China  
hktsang@ee.cuhk.edu.hk

**Abstract**—We have demonstrated a compact thermo-optic switch based on the differential effective thermo-optic coefficient of different waveguide supermodes. The extinction ratio exceeds 18 dB across a 40 nm wavelength range.

**Keywords**—silicon photonics, thermo-optic switch, programmable photonic integrated circuits (key words)

## I. INTRODUCTION

Variable optical splitters are essential elements of programmable photonic integrated circuits (PICs), which have found emerging applications in optical multimode communication systems [1], optical signal processing [2, 3], deep learning [4], and quantum information processing [5] and reconfigurable WDM filters [6]. Typically, variable optical splitters may be implemented by thermally tuned integrated Mach Zehnder interferometers (MZI). However, in programmable Mach-Zehnder interferometer meshes for unitary matrix multiplication systems, the number of required single MZI and total area rapidly scales up by  $\sim N^2$ , where  $N$  is the number of input data channels. Therefore, more compact optical splitters are needed to improve the scalability and reduce the total area and cost of the PIC. Previous approaches reported compact optical switches including the use of temperature gradients to tune the coupling of integrated directional couplers [7] implemented on the silicon-on-insulator (SOI) platform, but the tuned transmission cannot fully cover the on-off state. Phase-change materials have also been utilized to switch the optical power [8] with a compact layout and efficient transmission.

In this paper, we proposed a compact thermo-optic (TO) switch based on the use of the different effective TO coefficient experienced by a pair of supermodes in a combination of strip waveguide and slot waveguide. Specifically, two inputs of the switch are coupled into the strip waveguide mode and the slot waveguide mode. The accumulated phase difference between them may be tuned by an integrated metal heater embedded in the oxide above the waveguide. Unlike conventional MZI based TO switch where the footprint reduction is inherently limited by thermal crosstalk between two arms or thermal isolation trench size between two arms, the approach proposed here does not have such limitation and hence can achieve a compact footprint with a width of  $1.4\mu\text{m}$ . The length depends on the difference in effective TO coefficient and in this proof-of-concept

demonstration was  $267\mu\text{m}$ . We experimentally demonstrated complete on-off switching with  $P_{\pi}=39.6\text{mW}$  and an extinction ratio larger than 18dB over a 40nm bandwidth. The insertion loss was less than 1dB for the bar transmission and 3dB for cross transmission. To the best of our knowledge, this is the first time slot waveguide mode was used in an optical switch or variable optical splitter.

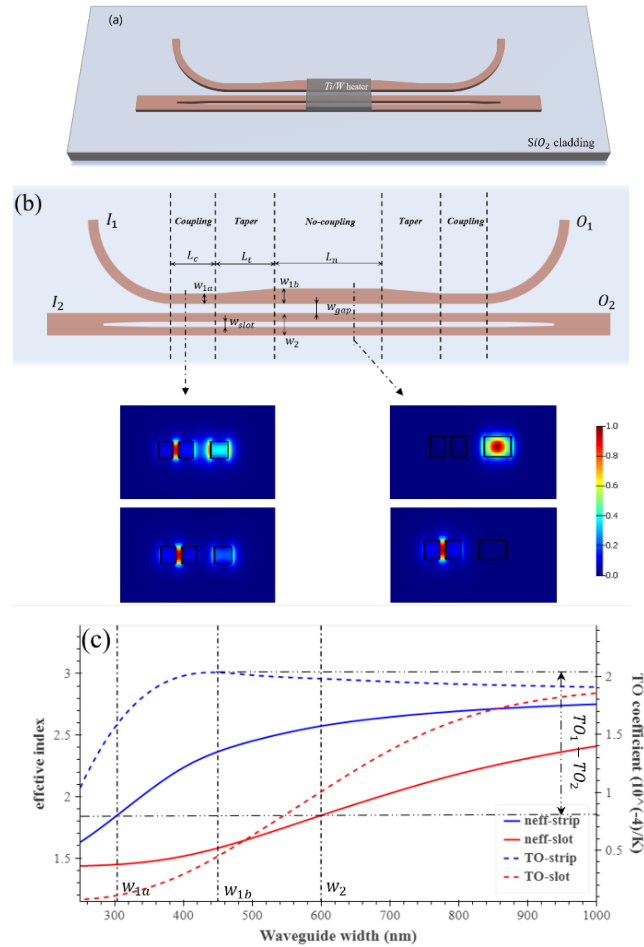


Fig. 1. (a) Schematic of the designed TO switch (not to scale); (b) Schematic of silicon layer pattern of the switch (not to scale), and electric field intensity profiles of supermodes in coupling and no-coupling regions; (c) Effective index and TO coefficient of strip waveguide and slot waveguide verses waveguide widths.

## II. DEVICE DESIGN AND ANALYSIS

The structure of the proposed thermal optical switch is shown in fig.1(a), which is composed of a strip waveguide, a slot waveguide and a titanium-tungsten metal heater on top of the silicon waveguides. The detailed silicon layer design is shown in fig.1(b). It comprises two coupling regions, two waveguide taper regions and a no-coupling region in the middle of the structure. The passive silicon layer of the proposed switch behaves like an asymmetric MZI. In the coupling region, the widths of the strip waveguide and the slot waveguide ( $w_{1a} = 304\text{nm}$  and  $w_2 = 600\text{nm}$ ) are designed to fulfill the phase matching condition. The fundamental modes of these two waveguides are designed to have the same effective index in the coupling region and thus switching of optical power between the waveguides is possible. The width of the strip waveguide is gradually increased from  $w_{1a}$  to  $w_{1b}$ , whereas the width of the slot waveguide remains unchanged. The lengths of the coupling region and the taper region ( $L_t = 1.655\mu\text{m}$  and  $L_c = 15\mu\text{m}$ ) are designed together to achieve 3dB power coupling between two waveguides at 1550nm wavelength, and ensure an adiabatic transition between the coupling and no-coupling regions where optical power leakage will not be caused. The electric field intensity profiles of the even and odd modes propagating in the coupling region are shown in inset of fig.1(b).

In the no-coupling region, the width of the strip waveguide is designed to be 450nm to fulfill the following two conditions. First, the power swapping need to be suppressed in this region. By properly increasing the strip waveguide width from  $w_{1a}$  to  $w_{1b} = 450\text{nm}$ , the effective indices of the strip and slot waveguide modes is well separated to break the phase matching condition, and optical power in two waveguides can propagate with a low crosstalk even when the gap between two waveguides is relatively narrow ( $w_{gap} = 350\text{nm}$ ). The electric field intensity profile of the two supermodes in no-coupling region are also shown in fig.1(b), where the field distributions are nearly the same as those of a single strip/slot waveguide. Second, a large difference in the effective thermo-optic (TO) coefficients between the two supermodes in the no-coupling region ( $TO_1 = \frac{dn_{eff1}}{dT}$ ,  $TO_2 = \frac{dn_{eff2}}{dT}$ ) is required to achieve efficient thermal tuning for designed switch. The width of the slot in the second waveguide is set to be 100nm, which make the fundamental mode power more confined in the slot region that is filled with silicon dioxide. Since silicon dioxide has a lower TO coefficient ( $TO_{SiO_2} = 0.8 \times 10^{-5}/K$ ) than silicon ( $TO_{Si} = 1.86 \times 10^{-4}/K$ ), and the optical confinement in silicon for slot mode is much lower than strip mode, the slot mode has a lower effective TO coefficient compared with the strip mode [9]. The phase difference between two supermodes when heater is turned on can be calculated as:

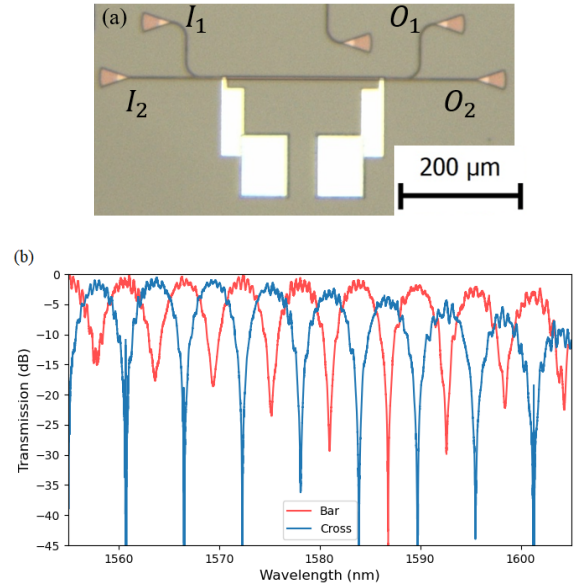
$$\Delta\phi = \Delta\phi_0 + \Delta\phi_1 = (n_{eff1} - n_{eff2}) \cdot L_{ht} + (TO_1 - TO_2) \cdot \Delta T \cdot L_{ht} \quad (1)$$

where  $\Delta\phi_0$  is inherent phase difference of the no-coupling region,  $\Delta\phi_1$  is thermally induced phase difference,  $\Delta T$  is the temperature difference in waveguides caused by the heater and  $L_{ht}$  is the heater length. It can be seen that the required temperature increase for a  $\pi$  phase difference is inversely proportional to  $(TO_1 - TO_2)$ , so the demand for efficient thermal tuning capability necessitate a large TO coefficient difference design between strip and slot waveguide mode.

Simulated TO coefficient variation verses waveguide width for strip and slot waveguides is shown in fig. 1(c), and  $w_{1b}$  is decided to be 450nm to meet the above two conditions. Besides,  $w_{1b}$  and  $w_2$  are also designed to avoid phase matching between fundamental slot mode and higher order strip modes. The total width of the no-coupling region is  $w_{1b} + w_2 + w_{gap} = 1.4\mu\text{m}$ , which has nearly same width as a multimode waveguide, and consumes far less chip area compared with a MZI based thermal switch that will require large arm spacing for heating crosstalk suppression or  $\sim 10\mu\text{m}$  wide thermal isolation trench in between. The length of the no-coupling region and heater ( $L_n$  and  $L_{ht}$ ) is  $234\mu\text{m}$  and  $200\mu\text{m}$ , respectively.

## III. FABRICATION AND EXPERIMENTAL RESULTS

The device was fabricated in silicon-on-insulator (SOI) platform for multi-project wafer run in Applied Nanotools Inc. [10], equipped with 220nm thick top silicon layer,  $2\mu\text{m}$  thick buried oxide and  $2.2\mu\text{m}$  thick oxide cladding. The silicon layer was patterned by electron beam lithography (EBL) technology and anisotropic inductively coupled plasma-reactive ion etching (ICP-RIE) process. Titanium/tungsten (Ti/W) metal and titanium/aluminum (Ti/Al) metal layers was utilized for high resistance heater and low resistance metal routing layer, respectively. Fig. 2(a) shows the microscope image of the fabricated switch. The spectrum was measured by a tunable laser source and a photodetector, utilizing a fast wavelength sweep controlling program. A mechanical polarization controller was connected between the laser and device under test (DUT) to adjust the polarization state of the incident light to couple to the TE mode. All the measurement instruments and DUT are linked using standard single mode fiber (SMF). A direct-current (DC) source was used to apply voltage on the fabricated Ti/W heater to provide thermal tuning for the variable optical splitter/switch. We also fabricated pairs of grating couplers (GCs) connected by single mode waveguide near the device to normalize out the GC coupling loss in the measurement.



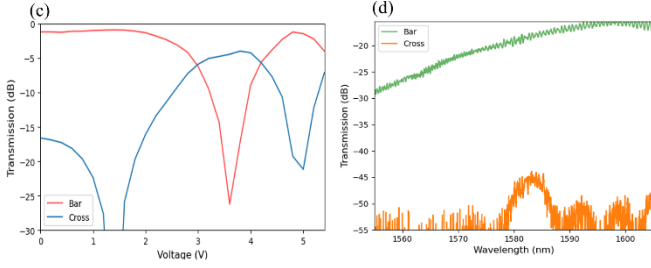


Fig. 2. (a) Microscope image of the fabricated TO switch; (b) Transmission spectrum of the TO switch when electric power is not applied to the heater. Bar:  $I_1-O_1$  transmission. Cross:  $I_1-O_2$  transmission; (c) Measured switch transmission versus voltage applied to the heater.

Fig. 2(b) shows the measured transmission spectra when no electric power is applied to the switch. The switch behaves like an asymmetric MZI with an free spectral range (FSR) of 5.8nm. The extinction ratio of the switch is measured to be  $>18$  dB in the wavelength range 1565-1605nm. The maximum extinction ratio was measured around 1585nm, which is red-shifted from the design target of 1550nm. The reason is due to fabrication tolerances, which is confirmed by a FDTD re-simulation of the coupling region by small increase in the waveguide width. Also, it can be observed that the loss gradually increases at longer wavelengths, and this is caused by the decreasing transmission efficiency of the strip-slot mode conversion at the input of the switch, and the slot mode is less confined in silicon at a longer wavelength which can lead to power leakage into the substrate [11]. This will also result in loss of the cross transmission higher than bar transmission especially at longer wavelength as shown in the measured spectra. The issue can be mitigated by using high efficiency strip-slot converter such as multimode interference coupler (MMI) based converter for mode conversion without increasing much device footprint [12]. Fig. 2(c) shows the measured voltage scanning result of the designed switch at 1584.3nm. The measured voltage at maximum/minimum transmission for bar transmission of the switch is 1.4V/3.6V. The resistance of heater is  $297.6\Omega$  at 2V voltage, and the power consumption for  $\pi$  switching is measured to be 39.6mW. The transmission loss at the highest extinction ratio wavelength is less than 1dB/3dB for bar/cross state. Fig. 2(d) shows the measured spectrum of the test structure where only no-coupling region waveguide of the switch are connected to input/output grating couplers. The power crosstalk is lower than 20dB for the whole measured bandwidth, demonstrating the asymmetric MZI-like behavior and effective prerequisite for the designed thermally phase tuning mechanism of the TO switch.

#### IV. CONCLUSION

We have designed and experimentally demonstrated a compact integrated variable optical splitter or optical switch.

Unlike conventional MZI based variable splitters, the device does not require the waveguides to operate at different temperatures. Instead the device proposed in this paper operates with both waveguides at the same temperature, and it is tuned by using the different effective TO coefficient experienced by different waveguide modes. The experimentally implemented device could be used as an optical switch with an extinction ratio higher than 18dB across a 40nm optical band. The heater power required for introducing  $\pi$  switching was 39.6mW. The device had a compact footprint of  $1.4 \times 267 \mu\text{m}^2$ . The performance can be further improved by using compact MMI based strip-slot mode converter and wideband fabrication robust strip-slot coupler. The proposed device can potentially be exploited in programmable PICs for better scalability and higher integration in future demonstrations.

#### ACKNOWLEDGMENT

This work was fully funded by Hong Kong RGC GRF grant 14207021. YQ and ZW also thank RGC for funding support from the Hong Kong PhD Fellowship scheme.

#### REFERENCES

- [1] A. Annoni, "Unscrambling light—automatically undoing strong mixing between modes", *Light: Science & Applications*, vol. 6, no. 12, pp. e17110–e17110, 2017.
- [2] D. Yi, Y. Wang and H. K. Tsang, "Multi-functional photonic processors using coherent network of micro-ring resonators", *APL Photonics*, vol. 6, no. 10, p. 100801, 2021.
- [3] D. Pérez-López, A. López, P. Dasmahapatra and J. Capmany, "Multipurpose self-configuration of programmable photonic circuits", *Nature Communications*, vol. 11, no. 1, 2020.
- [4] Y. Shen, "Deep learning with coherent nanophotonic circuits", *Nature Photonics*, vol. 11, no. 7, pp. 441–446, 2017.
- [5] N. C. Harris, "Linear programmable nanophotonic processors", *Optica*, vol. 5, no. 12, p. 1623, 2018.
- [6] J. Li, S. Yang, H. Chen and M. Chen, "Reconfigurable Rectangular Filter With Continuously Tunable Bandwidth and Wavelength," *IEEE Photonics Journal*, vol. 12, no. 4, Art no. 6601309, 2020.
- [7] P. Orlandi, F. Morichetti, M. J. Strain, M. Sorel, A. Melloni and P. Bassi, "Tunable silicon photonics directional coupler driven by a transverse temperature gradient", *Optics Letters*, vol. 38, no. 6, p. 863, 2013.
- [8] P. Xu, J. Zheng, J. K. Doylend and A. Majumdar, "Low-Loss and Broadband Nonvolatile Phase-Change Directional Coupler Switches", *ACS Photonics*, vol. 6, no. 2, pp. 553–557, 2019.
- [9] W. N. Ye, J. Micheland L. C. Kimerling, "Athermal High-Index-Contrast Waveguide Design", *IEEE Photonics Technology Letters*, vol. 20, no. 11, pp. 885–887, 2008.
- [10] Applied Nanotools Inc. <https://www.appliednt.com/>.
- [11] J. D. Sarmiento-Merenguel et al., "Controlling leakage losses in subwavelength grating silicon metamaterial waveguides", *Optics Letters*, vol. 41, no. 15, pp. 3443–3446, 2016.
- [12] Q. Deng, L. Liu, X. Li, and Z. Zhou, "Strip-slot waveguide mode converter based on symmetric multimode interference", *Optics Letters*, vol. 39, no. 19, pp. 5665–5668, 2014.